

Triangle Mesh Subdivision with Bounded Curvature and the Convex Hull Property

Charles Loop
cloop@microsoft.com

February 1, 2001

Technical Report
MSR-TR-2001-24

The masks for Loop's triangle subdivision surface algorithm are modified resulting in surfaces with bounded curvature and the convex hull property. New edge masks are generated by a cubic polynomial *mask equation* whose Chebyshev coefficients are closely related to the eigenvalues of the corresponding subdivision matrix. The mask equation is found to satisfy a set of smoothness constraints on these eigenvalues. We observe that controlling the root structure of the mask equation is important for deriving subdivision masks with non-negative weights.

Microsoft Research
Microsoft Corporation
One Microsoft Way
Redmond, WA 98052
<http://www.research.microsoft.com>

1 Introduction

Subdivision surfaces have become a popular geometric modeling primitive for representing smooth free-form shapes. Subdivision surfaces easily represent arbitrary topology surfaces and possess a simple, recursive, geometric construction algorithmic. This algorithm takes as input an initial *control mesh* and subdivides the faces and edges to form a new control mesh with more faces, edges, and vertices than the original while leaving the topology unchanged. By applying this procedure recursively, a smooth limit surface is obtained that is topologically equivalent to the original control mesh. This process is illustrated in Figure 1.

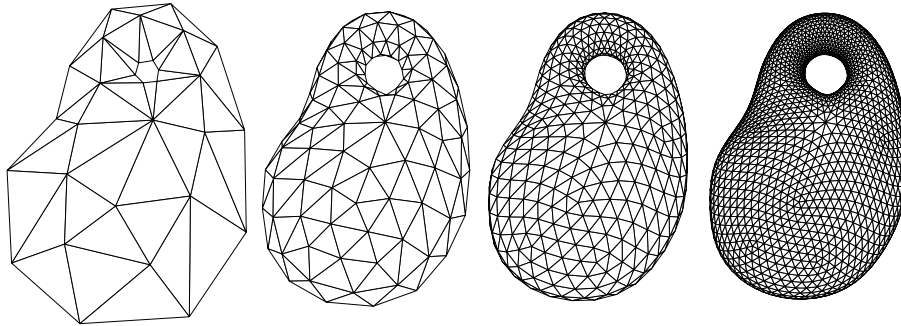


Figure 1: Initial control mesh (far left) and three iterations of Loop's subdivision surface algorithm.

While the original subdivision algorithms have proved a valuable tool for modeling arbitrary topology shapes, the surfaces generated by the original formulations may have unbounded curvatures. This defect can be removed by manipulating the spectrum of the subdivision operator. However, the important convex hull property may be lost. The contribution of this paper is a new technique for generating subdivision masks that obey well understood bounded curvature constraints without introducing negative weights. This technique can be summarized as follows: we replace the discrete cosine transform, that connects mask weights to eigenvalues, with Chebyshev polynomials to derive a cubic polynomial that we call a *mask equation*. We find this equation subject to tangent plane continuity and bounded curvature constraints, and we impose a special root structure that ensures non-negativity in the range of interest. The coefficients of the mask equation have a simple form, and the mask weights are found by evaluating this cubic polynomial. The result is an easy to implement algorithm that requires no deep understanding of subdivision matrix structure. We believe this approach may have value in general if negative weights are to be avoided in subdivision masks.

This paper is organized as follows. In Section 2, results relating to the smoothness of subdivision surfaces are discussed. In Section 3 we review Loop's

algorithm, and in Section 4 we outline our modifications to this algorithm. In Section 5 we review well understood subdivision matrix structure and develop a parameterized subdivision matrix. In Section 6, constraints on this parameterization sufficient for tangent plane continuity and bounded curvature are reviewed. In Section 7 we present a cubic polynomial mask equation that satisfies these constraints. Finally, Sections 8 and 9 present results and conclusions.

2 Background

The first subdivision surfaces were developed independently by Doo&Sabin [3] and Catmull&Clark [2]. These methods generalize the subdivision rules of bi-quadratic and bicubic tensor product B-Spline surfaces respectively. Loop[8] derived a triangle based subdivision surface by generalizing the subdivision rules for quartic box splines. These surfaces inherit the smoothness properties of their underlying polynomial splines at all but a finite number of extraordinary vertices. A control mesh vertex is *extraordinary* if it has irregular valence, otherwise it is *ordinary*. Ordinary vertices have valence 4 for rectangle based surfaces, or 6 for triangle based surfaces. The smoothness properties of a subdivision surface at points corresponding to extraordinary vertices are derived from the spectral properties of the subdivision operator[1, 4, 8].

Extraordinary vertices are isolated by expanding layers of *spline rings* as the subdivision level increases. Each spline ring is a collection of polynomial patches that parameterize the surface surrounding an extraordinary vertex. In studying the smoothness of subdivision surfaces at an extraordinary vertex, only a single generic spline ring of valence n need be considered. The subdivision operator takes one spline ring onto the next and is linear. A matrix \mathbf{A} that encodes this operator is known as a *subdivision matrix*. Since subdivision is affine invariant, \mathbf{A} will have a single dominant eigenvalue 1 with corresponding eigenvector $[1, 1, \dots, 1]^T$. For symmetric subdivision schemes, e.g. the methods of Doo&Sabin, Catmull&Clark, and Loop, \mathbf{A} will also have a pair of subdominant eigenvalues λ .

Reif[12] derived necessary and sufficient conditions for tangent plane (G^1) continuity by showing that the *characteristic map* defined by the pair of subdominant eigenvectors must be regular and injective. The characteristic map takes individual patch domains into a common xy -plane whose origin corresponds to the extraordinary vertex. Higher order smoothness properties are studied in terms of Taylor expansions over this plane. Necessary conditions for G^k continuity, for certain classes of subdivision surfaces, have been given by Prautzsch&Reif[9]. For curvature (G^2) continuity, in addition to G^1 continuity, the following must also hold:

- \mathbf{A} has a subsubdominant eigenvalue μ , where $|\mu| = \lambda^2$.
- If $\mathbf{A}v = \mu v$, then the surface defined by $v \in \text{span}(x^2, xy, y^2)$.

Prautzsch&Reif use a degree argument to show that no modification to the Catmull&Clark or Loop schemes can be used to construct G^2 continuous surfaces

with non-zero curvature at points corresponding to extraordinary vertices.

Despite the apparent failure to realize true curvature continuity, several authors[4, 8, 13] have noted the importance of the ratio $\lambda^2/|\mu|$ in controlling the divergence of the curvature at extraordinary vertices:

1. If $\lambda^2/|\mu| < 1$, then the curvature is unbounded
2. If $\lambda^2/|\mu| = 1$, then the curvature is bounded
3. If $\lambda^2/|\mu| > 1$, then the curvature is zero

Sabin[15] was the first to propose a bounded curvature subdivision surface algorithm; deriving a modified version of the Catmull&Clark algorithm. Prautzsch&Umlauf[10, 11] create modified versions of the Catmull&Clark and Loop algorithms with zero curvature at points corresponding to extraordinary vertices. Although these schemes are technically G^2 , introducing such *flat* spots on the surface is certainly undesirable. Moreover, their modifications lead to negative weights in the subdivision masks, violating the convex hull property. Holt[7] devised a bounded curvature subdivision algorithm based on Loop’s algorithm by finding an appropriate bounded curvature spectrum. Holt’s approach does not increase the support of the edge mask, and does not have the convex hull property for all valence. Zorin[17] has proposed a bounded curvature triangle subdivision scheme with non-negative weights by imposing a spectrum of the form $\lambda_k = (\frac{1}{2})^k$. This increases the support of edge masks, but the subdominant eigenvalue λ is fixed at $\frac{1}{2}$ for all valence (see Remark 1).

In this paper, we take advantage of property (2) to develop a modified version of Loop’s algorithm that has bounded curvature and non-negative weights. We choose the subdominant eigenvalue λ so that the characteristic maps are consistent with Loop’s algorithm; though this is not a requirement. Indeed, letting λ vary may be beneficial when constructing *fair* shapes. More importantly, we provide a general technique for deriving subdivision masks with non-negative weights.

3 Loop’s algorithm

Loop’s algorithm subdivides a triangulated control mesh by quadrisecting each face as shown in Figure 2. New vertices of the subdivided mesh are found as affine combinations of the vertices of the original control mesh. The weights associated with these combinations are called *masks*. The new vertices fall into two classes; those corresponding to vertices of the original control mesh, and those corresponding to edges of the original control mesh. The associated masks are referred to as *vertex masks* and *edge masks* respectively. Figure 3 depicts the two types of masks used in Loop’s algorithm.

A vertex mask assigns weight to an original mesh vertex, and the set of direct edge sharing neighbor vertices; the so-called *1-ring*. The weights used in the vertex mask are

$$\alpha = \left(\frac{3}{8} + \frac{1}{4} \cos \frac{2\pi}{n}\right)^2 + \frac{3}{8} \quad \text{and} \quad \beta = \frac{1}{n} (1 - \alpha),$$

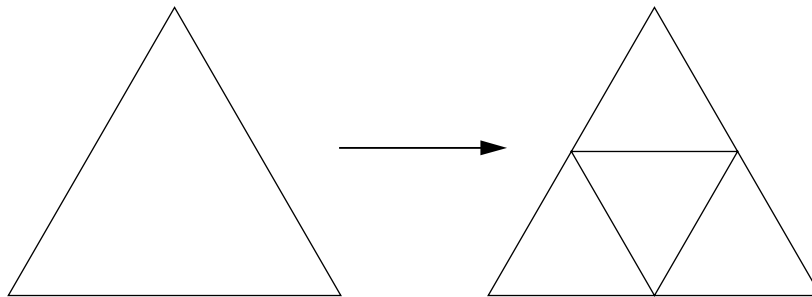


Figure 2: Quadrisection of a single triangular face.

where n is the valence of the vertex. The edge mask assigns weight to the vertices of the two triangles that share the edge, and do not depend on vertex valence.

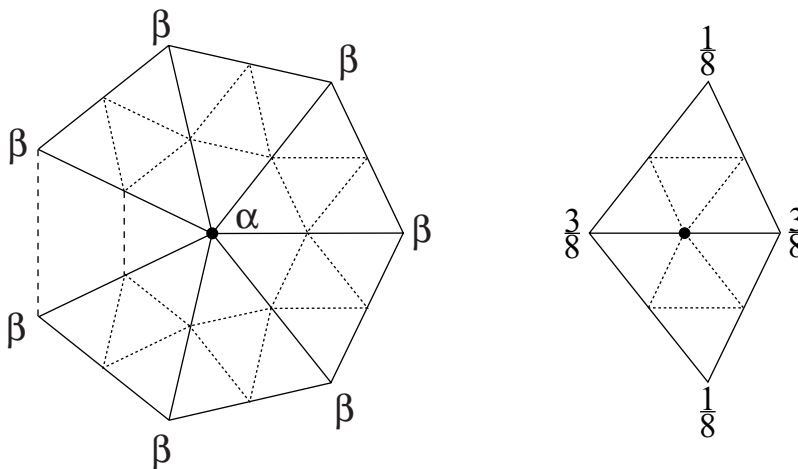


Figure 3: Vertex mask and edge mask used in Loop's algorithm.

Loop's algorithm is a generalization of binary subdivision of C^2 trilaterally symmetric quartic box splines[14]. If the initial control mesh is a regular triangulation (all vertices are valence 6), then the limit surface of Loop's algorithm is a quartic box spline with continuous curvatures.

4 A Modified Triangle Subdivision Algorithm

We propose a modified version of Loop's algorithm where the edge masks have larger support. The proposed edge mask is depicted in Figure 4. The mask

weights $1 - \lambda_0, \gamma_0, \dots, \gamma_{n-1}$ will form a partition of unity, so $\lambda_0 = \sum \gamma_i$. This is identical to the approach taken in [11, 17], however our method of deriving the weights γ_i is entirely different.

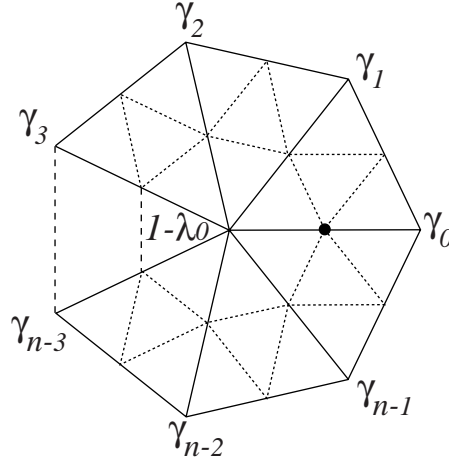


Figure 4: Modified edge mask for the new algorithm.

We point out that such a modified edge mask will be asymmetric with respect to the two incident vertices. That is, the position of a new mesh vertex associated with an edge will differ depending on which of the two incident vertices is used to determine the new edge mask. This ambiguity is handled by examining the valence of the two incident vertices:

- *If both vertices are ordinary, use the original edge mask.*
- *If one vertex is extraordinary, use the edge mask associated with that vertex.*
- *If both vertices are extraordinary, use both masks and average the result.*

Note that the last case above will only occur during the first level of subdivision, since all extraordinary vertices are surrounded by ordinary vertices after one iteration. This means that only edges that are incident on an extraordinary vertex will use a modified edge mask. A modified edge mask is determined by the valence n of the incident extraordinary vertex; rotated versions of a single edge mask are used to compute all the new edge points adjacent to the extraordinary vertex.

5 Subdivision Matrix Parameterization

The subdivision matrix, used to analyze the smoothness properties of a subdivision surface at an extraordinary vertex, transforms a spline ring at subdivision

level i to a spline ring at level $i + 1$. In the case of Loop's algorithm, the spline ring coefficients correspond to three rings of control mesh vertices surrounding an extraordinary vertex, a so-called β -ring. In fact, all of the large eigenvalues of a subdivision matrix (those of interest here) can be shown to come from the 1-ring. For this reason, modifications of the type to be considered here need only consider the 1-ring subdivision matrix and its eigen structure. The eigen decomposition of subdivision matrices is well understood[4]. We review the procedure here in order to define a particular subdivision matrix parameterization.

Let n be the valence of a generic extraordinary vertex and let $\alpha, \lambda_0, \lambda_1, \dots, \lambda_{n-1}$ be a set of scalar values. We define the matrix

$$\mathbf{Q} = \left[\begin{array}{c|cccc} \alpha & 1 - \alpha & 0 & \cdots & 0 \\ \hline 1 - \lambda_0 & \lambda_0 & 0 & \cdots & 0 \\ 0 & 0 & \lambda_1 & 0 & \cdots \\ \vdots & \vdots & & \ddots & \\ 0 & 0 & \cdots & 0 & \lambda_{n-1} \end{array} \right].$$

The 1-ring subdivision matrix \mathbf{S} is related to \mathbf{Q} by the following

$$\mathbf{S} = \mathbf{F}\mathbf{Q}\mathbf{F}^{-1},$$

where

$$\mathbf{F} = \left[\begin{array}{c|cccc} 1 & 0 & \cdots & 0 \\ \hline 0 & & & \\ \vdots & & \hat{\mathbf{F}} & \\ 0 & & & \end{array} \right] \quad \text{and} \quad \mathbf{F}^{-1} = \left[\begin{array}{c|cccc} 1 & 0 & \cdots & 0 \\ \hline 0 & & & \\ \vdots & & \hat{\mathbf{F}}^{-1} & \\ 0 & & & \end{array} \right]$$

are block diagonal matrices whose lower blocks are the $n \times n$ discrete fourier transform matrix and corresponding inverse defined

$$\hat{\mathbf{F}}_{j,k} = e^{\frac{2\pi i j k}{n}}, \quad \hat{\mathbf{F}}_{j,k}^{-1} = \frac{1}{n} e^{-\frac{2\pi i j k}{n}}, \quad j, k \in 0, \dots, n - 1.$$

The eigen structure of \mathbf{S} is the decomposition

$$\mathbf{S} = \mathbf{V}\mathbf{\Lambda}\mathbf{V}^{-1}$$

where $\mathbf{\Lambda}$ is a diagonal matrix of *eigenvalues*; \mathbf{V} and its inverse \mathbf{V}^{-1} are square matrices whose rows (resp. columns) are right (resp. left) *eigenvectors* of \mathbf{S} . These matrices are related to our parameterization as follows:

$$\mathbf{\Lambda} = \mathbf{G}^{-1}\mathbf{Q}\mathbf{G}, \quad \mathbf{V} = \mathbf{F}\mathbf{G}, \quad \text{and} \quad \mathbf{V}^{-1} = \mathbf{G}^{-1}\mathbf{F}^{-1},$$

where

$$\mathbf{G} = \left[\begin{array}{c|c} \hat{\mathbf{G}} & \mathbf{0} \\ \hline \mathbf{0} & \mathbf{I}_{n-1} \end{array} \right] \quad \text{and} \quad \mathbf{G}^{-1} = \left[\begin{array}{c|c} \hat{\mathbf{G}}^{-1} & \mathbf{0} \\ \hline \mathbf{0} & \mathbf{I}_{n-1} \end{array} \right]$$

are block diagonal matrices whose upper 2×2 blocks are defined

$$\hat{\mathbf{G}} = \begin{bmatrix} 1 & \frac{1-\alpha}{\lambda_0-1} \\ 1 & 1 \end{bmatrix} \quad \text{and} \quad \hat{\mathbf{G}}^{-1} = \frac{1}{2-\alpha-\lambda_0} \begin{bmatrix} 1-\lambda_0 & 1-\alpha \\ \lambda_0-1 & 1-\lambda_0 \end{bmatrix},$$

and whose lower block \mathbf{I}_{n-1} is the $(n-1) \times (n-1)$ identity matrix. The eigen decomposition of \mathbf{S} is thus written

$$\mathbf{S} = \mathbf{F}\mathbf{G}\mathbf{\Lambda}\mathbf{G}^{-1}\mathbf{F}^{-1} = \mathbf{F}\mathbf{Q}\mathbf{F}^{-1} = \left[\begin{array}{c|ccc} \alpha & \frac{1-\alpha}{n} & \dots & \frac{1-\alpha}{n} \\ 1-\lambda_0 & & & \\ \vdots & & \hat{\mathbf{S}} & \\ 1-\lambda_0 & & & \end{array} \right], \quad (1)$$

and

$$\mathbf{\Lambda} = \mathbf{G}^{-1}\mathbf{F}^{-1}\mathbf{S}\mathbf{F}\mathbf{G} = \mathbf{G}^{-1}\mathbf{Q}\mathbf{G} = \begin{bmatrix} 1 & 0 & 0 & \dots & 0 \\ 0 & \alpha + \lambda_0 - 1 & 0 & \dots & 0 \\ 0 & 0 & \lambda_1 & \dots & 0 \\ \vdots & & & \ddots & 0 \\ 0 & \dots & & 0 & \lambda_{n-1} \end{bmatrix} \quad (2)$$

where

$$\hat{\mathbf{S}} = \hat{\mathbf{F}}\text{diag}(\lambda)\hat{\mathbf{F}}^{-1} = \text{circ}(\gamma), \quad (3)$$

and

$$\lambda = [\lambda_0, \dots, \lambda_{n-1}], \quad \gamma = [\gamma_0, \dots, \gamma_{n-1}].$$

The parameters $\lambda_0, \dots, \lambda_{n-1}$ are the eigenvalues of $\hat{\mathbf{S}}$, the lower right $n \times n$ block of \mathbf{S} in Equation (1). Note that $\hat{\mathbf{S}}$ is a circulant matrix constructed from the edge mask weights $\gamma_0, \dots, \gamma_{n-1}$. The parameter α is the central weight of the corresponding vertex mask; this value will differ (in general) from the value used in Loop's algorithm.

6 Parameterization Constraints

The parameterization of \mathbf{S} we consider characterizes a large space of possible subdivision matrices. We reduce the size of this space by imposing constraints on the parameters $\alpha, \lambda_0, \dots, \lambda_{n-1}$.

6.1 Symmetry

We consider only symmetric subdivision schemes, so $\hat{\mathbf{S}}$ will be a circulant matrix consisting of real values γ , if λ is symmetric. That is, the elements of λ are matched pairwise:

$$\lambda_1 = \lambda_{n-1}, \lambda_2 = \lambda_{n-2}, \dots, \lambda_{\lfloor \frac{n}{2} \rfloor} = \lambda_{\lceil \frac{n}{2} \rceil}.$$

When n is even, $\lambda_{\frac{n}{2}}$ is not matched. Note that if λ is not symmetric, γ may not be real. Assuming symmetry, Equation (3) can be rewritten

$$\hat{\mathbf{S}} = \text{circ}(\gamma) \quad \text{where} \quad \gamma = \lambda \mathbf{C} \quad \text{and} \quad \mathbf{C}_{i,j} = \frac{1}{n} \cos \frac{2\pi ij}{n}. \quad (4)$$

That is, γ and λ are related by the $n \times n$ *discrete cosine transform* matrix \mathbf{C} .

6.2 Convergence

We guarantee that the subdivision process will converge to a well defined surface by requiring that all the eigenvalues of \mathbf{S} be less than or equal to 1 in absolute value. From Equation (2) the eigenvalues of \mathbf{S} are

$$1, \alpha + \lambda_0 - 1, \lambda_1, \lambda_2, \dots, \lambda_{n-1}.$$

The constraints for convergence are therefore

$$1 > |\alpha + \lambda_0 - 1|, \quad \text{and} \quad 1 > |\lambda_i|, \quad i = 1, \dots, n-1. \quad (5)$$

6.3 Continuous tangent plane

The subdivision surface will converge to a common tangent plane at each extraordinary vertex, if there exist a pair of subdominant eigenvalues such that the characteristic map defined by the corresponding eigenvectors is regular and injective. The characteristic map for subdivision schemes have been extensively studied[5, 16]. We leverage these results by constraining the subdominant eigenvalue pair λ_1 and λ_{n-1} to be consistent with Loop's algorithm. Prautzsch&Umlauf take the same approach and prove equivalence of the characteristic map[11]. The constraints for tangent plane continuity are therefore

$$\lambda_1 = \lambda_{n-1} = \frac{3}{8} + \frac{1}{4} \cos \frac{2\pi}{n}, \quad \text{and} \quad \lambda_1 > |\lambda_i|, \quad i = 2, \dots, n-2. \quad (6)$$

Remark 1 *Selecting λ_1 so the characteristic maps are consistent with Loop's algorithm is not required. Studying the qualitative effect of various choices for λ_1 is beyond the scope of this paper, though this effect can be significant. We have no compelling reason to deviate from the generally accepted value provided by Loop's algorithm. We point out however, that the flexibility to do so is available.*

6.4 Bounded curvature

The subdivision surface will have bounded curvature if

$$\lambda_2 = \lambda_{n-2} = \alpha + \lambda_0 - 1 = \lambda_1^2, \quad \text{and} \quad \lambda_2 > |\lambda_i|, \quad i = 3, \dots, n-3, \quad (7)$$

where $n \geq 5$ (we handled cases where $n < 6$ separately). This will endow \mathbf{S} with a subsubdominant eigenvalue of geometric and algebraic multiplicity 3. While this multiplicity of the subsubdominant eigenvalue is a stronger condition than required for bounded curvature, it is a necessary condition for non-degenerate curvature continuity (i.e., where the osculating paraboloid can span all quadratics). Note that Equations (6) and (7) imply (5); that is, tangent plane continuity and bounded curvature imply convergence.

6.5 Non-negative weights

We insist that \mathbf{S} be non-negative. This will guarantee that the limit surface is within the convex hull of the control mesh. From Equations (1) and (4), it follows that \mathbf{S} will be non-negative if and only if

$$\gamma_i = [\lambda \mathbf{C}]_i \geq 0, \quad i = 0, \dots, n-1; \quad 0 \leq \alpha \leq 1; \quad \text{and} \quad \lambda_0 \leq 1. \quad (8)$$

In the next section, we present our approach to satisfying the tangent plane, bounded curvature, and non-negative weight constraints simultaneously.

7 A Mask Equation

We want the product $\gamma = \lambda \mathbf{C}$, subject to constraints on λ , so that γ is non-negative. Our approach is to convert the mask weights from a discrete set to a continuous function that is evaluated n times to recover γ .

Expanding Equation (8), we write

$$\gamma_i = \frac{1}{n} \sum_{j=0}^{n-1} \lambda_j \cos \frac{2\pi i j}{n},$$

which we convert to the continuous function

$$\gamma(\theta) = \frac{1}{n} \sum_{j=0}^{n-1} \lambda_j \cos(j\theta)$$

since $\gamma_i = \gamma(\frac{2\pi i}{n})$, $i = 0, \dots, n-1$. We make the substitution $\theta = \arccos u$ and define

$$M_n(u) = \sum_{i=0}^{\lfloor \frac{n}{2} \rfloor} x_i T_i(u) \quad (9)$$

where $T_i(u)$ is the i^{th} Chebyshev polynomial; by definition, $T_k(\cos \theta) \equiv \cos(k\theta)$. The Chebyshev coefficients x_i and parameters λ_i are related by

$$x_i = \frac{1}{n} \begin{cases} \lambda_0 & \text{if } i = 0, \\ \lambda_{\frac{n}{2}} & \text{if } i = \frac{n}{2} \text{ and } n \text{ is even,} \\ 2\lambda_i & \text{otherwise.} \end{cases} \quad (10)$$

Example 2 Consider the regular case $n = 6$. Decomposition of the regular subdivision matrix leads to

$$\lambda = \left\{ \frac{5}{8}, \frac{1}{2}, \frac{1}{4}, \frac{1}{8}, \frac{1}{4}, \frac{1}{2} \right\}.$$

From this

$$\begin{aligned} M_6(u) &= \frac{1}{6} \left[\frac{5}{8} T_0(u) + T_1(u) + \frac{1}{2} T_2(u) + \frac{1}{8} T_3(u) \right] \\ &= \frac{5}{48} + \frac{1}{6} u + \frac{1}{12} (2u^2 - 1) + \frac{1}{48} (4u^3 - 3u) \\ &= \frac{1}{12} (1 + u) \left(\frac{1}{2} + u \right)^2 \end{aligned}$$

We verify this result by evaluating $M_6(\cos \frac{\pi i}{3})$, $i = 0, \dots, 5$ to get the edge mask values $\{\frac{3}{8}, \frac{1}{8}, 0, 0, 0, \frac{1}{8}\}$.

7.1 The General Form

We would like a general mask equation for arbitrary $n \geq 6$. We propose

$$\boxed{M_n(u) = a(1+u)(u+b)^2} \quad (11)$$

This cubic polynomial has a single root at $u = -1$, and a double root at $u = -b$. The root structure of $M_n(u)$ is the key to avoiding negative mask weights, since $a > 0$ and $b > -1$ in Equation (11) implies that $M_n(u)$ is non-negative in the interval $-1 \leq u \leq 1$ (i.e., the range of $\cos \theta$).

We proceed to solve for a and b subject to the constraints. Mask Equation (11) is expressed in terms of the Chebyshev basis as follows

$$M_n(u) = [1, u, 2u^2 - 1, 4u^3 - 3u] \begin{bmatrix} a(\frac{1}{2} + b(1+b)) \\ a(\frac{3}{4} + b(2+b)) \\ a(\frac{1}{2} + b) \\ \frac{1}{4}a \end{bmatrix}. \quad (12)$$

The tangent plane and bounded curvature constraints (Equations (6), (7)), are related to the Chebyshev coefficients (Equation (10)) by

$$x_1 = \frac{2}{n}\lambda_1 \quad \text{and} \quad x_2 = \frac{2}{n}\lambda_1^2.$$

This gives us two equations in two unknowns

$$\begin{aligned} \frac{2}{n}\lambda_1 &= a\left(\frac{3}{4} + b(2+b)\right), \\ \frac{2}{n}\lambda_1^2 &= a\left(\frac{1}{2} + b\right). \end{aligned}$$

These are solved with the aid of the quadratic formula leading to the unique solution

$$a = \frac{2\lambda_1^3}{n(1-\lambda_1)}, \quad (13)$$

$$b = \frac{1}{\lambda_1} - \frac{3}{2}, \quad (14)$$

where $\lambda_1 = \frac{3}{8} + \frac{1}{4}\cos \frac{2\pi}{n}$ is the imposed subdominant eigenvalue of the subdivision matrix. Equations (13) and (14) are substituted into (11), which is then evaluated at $u = \cos \frac{2\pi i}{n}$, $i = 0, \dots, n-1$ to obtain the mask weights.

It remains to determine the central weights of the modified masks. By construction, we know that $\lambda_0 = \sum \gamma_i$. However, we also have a relation (Equations (10) and (12)) between λ_0 and the Chebyshev coefficient x_0 , that is

$$x_0 = \frac{1}{n}\lambda_0 = a\left(\frac{1}{2} + b(1+b)\right).$$

This implies

$$\lambda_0 = \frac{\lambda_1 (4 + \lambda_1 (5\lambda_1 - 8))}{2(1 - \lambda_1)}. \quad (15)$$

The central weight for the edge mask is $1 - \lambda_0$, and we see from Equation (7) that the central weight for the vertex mask is found by

$$\alpha = 1 - \lambda_0 + \lambda_1^2. \quad (16)$$

Example 3 Consider the case $n = 8$. Substituting $\lambda_1 = \frac{3+\sqrt{2}}{8}$ into Equations (13) and (14) we get

$$a = \frac{283 + 190\sqrt{2}}{5888} \quad \text{and} \quad b = \frac{27 - 16\sqrt{2}}{14}.$$

Next, we use these values and evaluate Equation (11) at $u = \cos \frac{\pi i}{4}, i = 0, \dots, 7$ to get the weights

$$\gamma = \{0.32273792, 0.16623202, 0.00914020, 0.00427714, 0.0, \dots\}.$$

We use (15) and (16) to determine that $\lambda_0 = 0.68203664$, and $\alpha = 0.62242088$.

By construction, all constraints have been satisfied; though we have yet to show that $\lambda_2 > |\lambda_i|, i = 3, \dots, n - 3$ (see Equation (7)). From Equations (10) and (12) we see that

$$x_3 = \frac{2}{n}\lambda_3 = \frac{1}{4}a, \quad (17)$$

and $\lambda_i = 0, i = 4, \dots, n - 4$ (for $n > 6$). To verify that $\lambda_2 > |\lambda_3|$, we combine (13) and (17) to get

$$\lambda_3 = \frac{\lambda_1^3}{4(1 - \lambda_1)}.$$

Since $\lambda_2 = \lambda_1^2$, it follows that $\lambda_2 > \lambda_3$ so long as $0 < \lambda_1 < \frac{4}{5}$. This is clearly the case for our particular choice $\lambda_1 = \frac{3}{8} + \frac{1}{4}\cos \frac{2\pi}{n}$, since in the limit as $n \rightarrow \infty$, $\lambda_1 \rightarrow \frac{5}{8}$. Note that $a \rightarrow 0$ and $b \rightarrow \frac{1}{10}$ as $n \rightarrow \infty$; this indicates that a is positive for all valence and the mask equation is well defined.

7.2 Cases $n < 6$

We now consider mask equations for the cases where $n = 3, 4$, and 5 . These require special treatment since appropriate mask equations will differ from the general form. When $n < 6$, λ_3 does not exist, so the mask equation does not have a cubic term. Similarly, when $n = 3$ there is no quadratic term. In the cases $n = 3$ and $n = 4$, the multiplicity of the subsubdominant eigenvalue is reduced, altering the systems to be solved. However, replacing the discrete cosine transform with Chebyshev polynomials still works and mask equations satisfying the constraints can be found. These are summarized in Table 7.2.

n	$M_n(u)$	λ_0	α
3	$\frac{1}{6}(\frac{5}{4} + u)$	$\frac{5}{8}$	$\frac{7}{16}$
4	$\frac{1}{2}(\frac{1}{2} + \frac{3}{8}u)^2$	$\frac{41}{64}$	$\frac{1}{2}$
5	$\frac{3+\sqrt{5}}{32}(\frac{5-\sqrt{5}}{5} + u)^2$	$\frac{31+5\sqrt{5}}{64}$	$\frac{81-5\sqrt{5}}{128}$

Note that the case $n = 3$ coincides with Loop’s algorithm.

7.3 Exact Evaluation

In practice, it is sometimes useful to compute points on the surface exactly. This can be done using a 1-ring mask derived from the 1st right eigenvector (see Section 5). Such a mask will have a central weight

$$\tau = \frac{1 - \lambda_0}{2 - \alpha - \lambda_0},$$

the remaining n weights will be $\frac{1}{n}(1 - \tau)$. A surface normal can be found by taking a cross product of the pair of vectors found by masks derived from the 2nd and 3rd right eigenvectors[6]

8 Results

The surfaces generated by the proposed algorithm demonstrate a visibly smoother appearance compared to surfaces obtained by Loop’s subdivision surface algorithm. Figure 5 shows a comparison of the old and new algorithms for various control meshes. The differences are subtle when vertex valence is low. By shading surfaces with Gauss curvature mapped to color, the difference become more apparent. The plots in Figure 5 use red for positive curvature, green for zero curvature, and blue for negative curvature. The scale and range of curvatures have not been given as these plots are intended for side-by-side comparison, with identical color mappings for shapes with the same control mesh.

In Figure 5a we see a slight change in the curvature plots near the extraordinary vertices. The control mesh in Figure 5b is an icosahdron; we see a more uniform distribution of curvature using the new algorithm and the resulting shape more sphere-like. The result of to the new algorithm becomes more obvious as vertex valence increases. Figures 5c and 5d show a cone-like shape with a vertex of valance 13, and a saddle-like shape with a vertex of valance 18, respectively. Notice the behavior, as subdivision level increases, of the 1-rings of the extraordinary vertices. For the new algorithm, the 1-ring is clearly getting smoother faster. This property is due to the increase in the support of the edge mask.

9 Conclusions

We have presented a modified version of Loop’s triangle subdivision surface algorithm with bounded curvature and the convex hull property. This new

algorithm uses edge masks with larger support, whose weights are generated by a cubic polynomial mask equation. A close relationship between the Chebyshev coefficients of this mask equation and the eigenvalues of the corresponding 1-ring subdivision matrix was established. Using this relationship, constraints on the eigenvalues sufficient for tangent plane continuity and bounded curvature are satisfied. We guarantee non-negativity of the mask equation by a simple root structure that does not allow zero crossings in the interval $-1 \leq u \leq 1$.

The convex hull property is important and desirable for surfaces in Computer Aided Geometric Design. We have demonstrated a relationship between subdivision masks and their associated spectrum involving a connection between the discrete cosine transform and Chebyshev polynomials. We use a continuous polynomial function called a mask equation to represent the transformation from the frequency to the spatial domain. Controlling the root structure of such a polynomial mask equation may be useful in general for deriving subdivision masks that are guaranteed not to have negative weights.

Acknowledgements

I wish to thank Kirk Olynyk for many helpful discussions and insights.

References

- [1] A. Ball and D. Storry. Conditions for tangent plane continuity over recursively generated b-spline surfaces. *ACM Transactions on Graphics*, 7(2):83–102, 1988.
- [2] E. Catmull and J. Clark. Recursively generated B-spline surfaces on arbitrary topological meshes. *Computer Aided Design*, 10(6):350–355, 1978.
- [3] D. Doo. A subdivision algorithm for smoothing down irregularly shaped polyhedrons. In *Proceedings on Interactive Techniques in Computer Aided Design, Bologna, Italy*, pages 157–165. IEEE, 1978.
- [4] D. Doo and M. Sabin. Behaviour of recursive division surfaces near extraordinary points. *Computer Aided Design*, 10(6):356–360, 1978.
- [5] G. Umlauf. Analyzing the characteristic map of triangular subdivision schemes. *Constructive Approximation*, 16(1):145–155, 2000.
- [6] M. Halstead, M. Kass, and T. DeRose. Efficient, fair interpolation using catmull-clark surfaces. In *SIGGRAPH 93 Conference Proceedings*, Annual Conference Series, pages 35–44. ACM SIGGRAPH, Addison Wesley, 1993.
- [7] F. Holt. Toward a curvature-continuous stationary subdivision algorithm. *Z. Angew. Math. Mech.*, Berlin, 76(1):423–424, 1996.

- [8] C. Loop. Smooth subdivision surfaces based on triangles. Master's thesis, University of Utah, 1987.
- [9] H. Prautzsch and U. Reif. Necessary conditions for subdivision surfaces. 1996. <http://i33www.ira.uka.de>.
- [10] H. Prautzsch and G. Umlauf. A G^2 -subdivision algorithm. In G. Farin, H. Bieri, G. Brunnet, and T. DeRose, editors, *Geometric Modelling*, volume 13 of Computing suppl. Springer-Verlag, 1998.
- [11] H. Prautzsch and G. Umlauf. Improved triangular subdivision schemes. In F. Wolter and N. Patrikalakis, editors, *Computer Graphics International 1998*, pages 626–632. IEEE Computer Society, June 1998.
- [12] U. Reif. A unified approach to subdivision algorithms near extraordinary vertices. *Computer Aided Geometric Design*, 12:153–174, 1995.
- [13] U. Reif and P. Schröder. Curvature smoothness of subdivision surfaces. Technical Report TR-00-03, Caltech, 1999.
- [14] M. Sabin. *The use of piecewise forms for the numerical representation of shape*. PhD thesis, Hungarian Academy of Sciences, Budapest, Hungary, 1976.
- [15] M. Sabin. Cubic recursive division with bounded curvature. In P Laurent, A Le Méhauté, and L. Schumaker, editors, *Curves and Surfaces*, pages 411–414, Boston, 1991. Academic Press.
- [16] J. Schweitzer. Analysis and application of subdivision surfaces. Technical Report UW-CSE-96-08-02, University of Washington, 1996.
- [17] D. Zorin. *Stationary Subdivision and Multiresolution Surface Representations*. PhD thesis, California Institute of Technology, 1998.

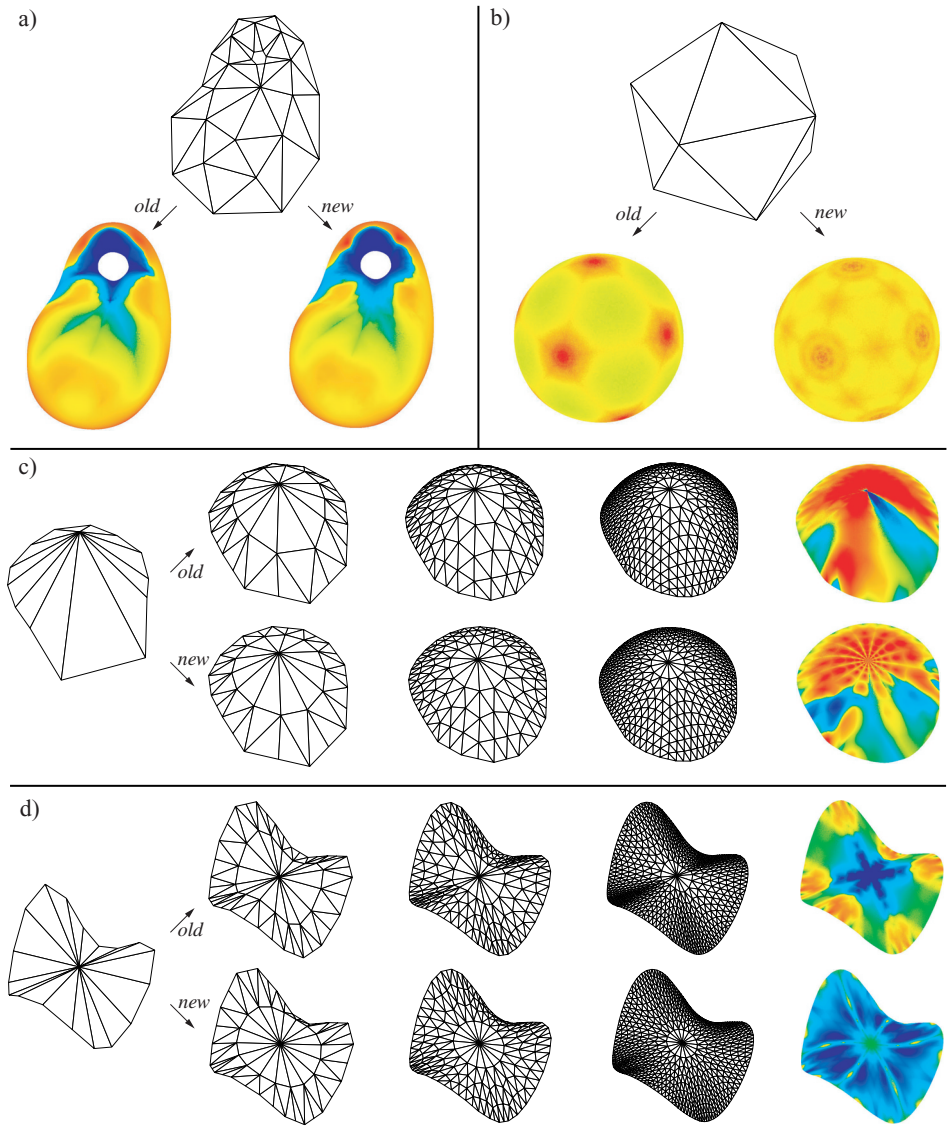


Figure 5: Results comparing the *old* version of Loop's algorithm to the *new* algorithm